Boise State University

ScholarWorks

Civil Engineering Faculty Publications and Presentations

Department of Civil Engineering

9-2023

Shrinkage and Consolidation Characteristics of Chitosan-Amended Soft Soil: A Sustainable Alternate Landfill Liner Material

Romana Mariyam Rasheed
TKM College of Engineering

Arif Ali Baig Moghal
National Institute of Technology Warangal

Sai Sampreeth Reddy Jannepally
National Institute of Technology Warangal

Ateekh Ur Rehman
King Saud University

Bhaskar C. S. Chittoori
Boise State University

buildings

MDPI

Article

Shrinkage and Consolidation Characteristics of Chitosan-Amended Soft Soil—A Sustainable Alternate Landfill Liner Material

Romana Mariyam Rasheed [1], Arif Ali Baig Moghal [2,*], Sai Sampreeth Reddy Jannepally [2], Ateekh Ur Rehman [3] and Bhaskar C. S. Chittoori [4]

[1] Department of Civil Engineering, TKM College of Engineering, Kollam 691005, India; romanamrasheed@tkmce.ac.in or rm712020@student.nitw.ac.in
[2] Department of Civil Engineering, National Institute of Technology Warangal, Warangal 506004, India; sjce21212@student.nitw.ac.in
[3] Department of Industrial Engineering, College of Engineering, King Saud University, Riyadh 11421, Saudi Arabia; arehman@ksu.edu.sa
[4] Department of Civil Engineering, Boise State University, Boise, ID 83725, USA; bhaskarchittoori@boisestate.edu
* Correspondence: baig@nitw.ac.in or reach2arif@gmail.com; Tel.:+91-9989677217

Abstract: Kuttanad is a region that lies in the southwest part of Kerala, India, and possesses soft soil, which imposes constraints on many civil engineering applications owing to low shear strength and high compressibility. Chemical stabilizers such as cement and lime have been extensively utilized in the past to address compressibility issues. However, future civilizations will be extremely dependent on the development of sustainable materials and practices such as the use of bio-enzymes, calcite precipitation methods, and biological materials as a result of escalating environmental concerns due to carbon emissions of conventional stabilizers. One such alternative is the utilization of biopolymers. The current study investigates the effect of chitosan (biopolymer extracted from shrimp shells) in improving the consolidation and shrinkage characteristics of these soft soils. The dosages adopted are 0.5%, 1%, 2%, and 4%. One-dimensional fixed ring consolidation tests indicate that consolidation characteristics are improved upon the addition of chitosan up to an optimum dosage of 2%. The coefficient of consolidation increases up to seven times that of untreated soil, indicating the acceleration of the consolidation process by incorporating chitosan. The shrinkage potential is reduced by 11% after amendment with 4% chitosan and all the treated samples exhibit zero signs of curling. Based on the findings from consolidation and shrinkage data, carbon emission assessments are carried out for a typical landfill liner amended with an optimum dosage of chitosan. In comparison to conventional stabilizers like cement and lime, the results indicate that chitosan minimized carbon emissions by 7.325 times and 8.754 times, respectively.

Keywords: carbon footprint; chitosan; coefficient of consolidation; compression index; soft soil

check for updates

Citation: Rasheed, R.M.; Moghal, A.A.B.; Jannepally, S.S.R.; Rehman, A.U.; Chittoori, B.C.S. Shrinkage and Consolidation Characteristics of Chitosan-Amended Soft Soil—A Sustainable Alternate Landfill Liner Material. *Buildings* **2023**, *13*, 2230. https://doi.org/10.3390/buildings13092230

Academic Editor: Junjie Zeng

Received: 8 August 2023
Revised: 23 August 2023
Accepted: 30 August 2023
Published: 31 August 2023

Copyright: © 2023 by the authors. Licensee MDPI, Basel, Switzerland. This article is an open access article distributed under the terms and conditions of the Creative Commons Attribution (CC BY) license (https://creativecommons.org/licenses/by/4.0/).

1. Introduction

Soft soil deposits pose severe constraints to the infrastructural development of any region. Some of these deposits undergo excessive settlements owing to their poor geotechnical characteristics [1]. The Kuttanad region is a stretch of low-lying land on the west coast of India and comprises silt and clay fraction [2]. A major portion of the region remains submerged during the monsoon season every year [3]. The behavior of these soft soils is predominantly dependent on the mineral type and microstructural arrangement. The unique structure developed by the insitu soil depends on the depositional environment and post-diagenetic process, which contribute additional strength and stiffness in comparison to remolded soil [4]. Amelioration with chemical amendments such as fly ash, cement, lime, nano calcium silicate, coal gangue, ground granulated blast furnace slag, nano-chemicals

like terrasil, and fiber-reinforced lime has proven their effectiveness in improving the properties of soft soils globally [5–19].

Several studies in the past have established the presence of organic matter in the deposits found in the Kuttanad region [20,21]. The studies have confirmed the presence of montmorillonite, hydromica, kaolinite, quartz, and possibly traces of gibbsite, chlorite, feldspar, and amphibole in the soil [21]. From a geotechnical standpoint, these clays are unfavorable due to their high compressibility, low shear strength, high permeability, and high proportion of organic content [22]. Lack of proper engineering judgment in the past has led to the collapse of embankments and bridges in this region [23]. Consequently, in-depth research on organic clays is necessary to successfully address unfavorable ground conditions. The inclusion of coir geotextile accelerated the consolidation in a shorter period and reduced the chances of premature failure [24]. Other techniques attempted to stabilize and mitigate the vulnerability of these deposits comprise the precompression techniques [25], stone columns [26], lime columns [27], and fiber reinforcement [28]. Amendments with lime, fly ash [29], and cement [21] have also modified the engineering properties of Kuttanad soil considerably.

However, chemical stabilization techniques have been showing detrimental effects on soil and the environment in the form of reduced soil plasticity, water pollution, deteriorating flora and fauna, and emissions of carbon monoxide, carbon dioxides, methane, and nonmethane volatile organic compounds [30]. With sustainability as the core concern in many engineering applications, materials such as calcite precipitation [31,32], biopolymers [33,34], etc., have come into practice. Owing to the controlled environment required for microbial growth and the cost of enzymes used for calcite precipitation, biopolymers can be preferred. Successful results were seen when several biopolymers, including guar gum, xanthan gum, agar gum, gellan gum, dextran, β-glucan, Persian gum, alginate gum, chitosan, polyhydroxy butyrate, polyglutamic acid, casein, etc., were applied to various types of soil [35–45].

The consolidation and shrinkage characteristics of organic soils bear significance in the performance of the soil. There have been studies conducted to assess the consolidation characteristics of soft soils using biopolymers. Tests conducted on montmorillonite and kaolinite using 1% and 1.5% of xanthan gum revealed the formation of new cementitious products formed as a result of the interaction between xanthan gum and soil particles. This led to the bridging between soil particles and the strengthening of bonds. The extended curing period of 90 days led to a reduction in compression and swelling indices by more than 50% [46]. The amendment of clayey soil with low plasticity using carboxyl methyl cellulose reduced the void ratio from 0.6 to 0.2 at a dosage of 5% [47]. Another issue that persists in a compacted clay liner is desiccation cracking due to internal and external circumstances in the final cover system, which leads to rainfall infiltration and affects the structural integrity. The permeability of the system increases by three orders of magnitude in such cases and leads to inefficiency. The soil may even exhibit curling up (convex) or curling down (concave) behavior during the process of shrinkage or desiccation cracking, especially in remolded conditions. A non-homogeneous distribution of particles, layer thickness, liquid limit, plastic limit, hydraulic conductivity, lift-off height, curvature, and soil type will influence the curling characteristics [48]. Amendments such as lime and cement have been introduced to fine-grained soil in the past to satisfy strength, and settlement criteria and offer resistance against cracking. However, the performance of these materials has been insufficient in satisfying the desired requirements. Recently, biopolymers have been incorporated to control desiccation cracking in soft soils. Low and high plastic clays amended with guar gum and xanthan gum have reduced the shrinkage potential [38,49].

Another novel material named chitosan is derived from the exoskeleton of marine waste and has been widely employed in the field of geoenvironmental engineering. Chitosan has exhibited a remarkable performance in heavy metal retainment and has served as an effective adsorbent in soil and water remediation [50–52]. Recent works using chi-

tosan have explored the possibility of soil amelioration [53]. Chitosan has proved to be an efficient amendment for the long-term strength of sand and the short-term strength of clay. While the mechanism of improvement for the chitosan–clay mix can be attributed to the electrostatic force of attraction, the sandy soils are bridged by the chitosan gel formed between them [54]. The dissolution of chitosan in acetic acid renders it cationic and cohesive in nature. The chitosan hydrogel formed will dehydrate to form fibers with time and bridge the soil particles, leading to a stable clayey structure [55]. The aggregated and flocculated structure induced by chitosan in kaolinite creates a rigid structure and leads to an elevated strength performance. However, higher dosages facilitate lubrication among particles and reduce cohesion, leading to a reduced compressive strength [56]. The literature review on chitosan-amended soils revealed that most of the studies evaluated the strength characteristics of cohesionless and cohesive soils. Seldom researchers have investigated the modification in compressibility and shrinkage properties of fine-grained soils utilizing chitosan [57].

The goal of the United Nations to integrate the 17 Sustainable Development Goals by 2030 has prompted geotechnical engineers to undertake the sustainability assessment for the works being carried out. Seldom works in the field of geotechnical engineering have conducted carbon emission analysis. In this regard, it becomes imperative to critically evaluate the carbon footprint of the various materials utilized in ground improvement works. The current study investigates the influence of a polysaccharide-based biopolymer derived from shrimp shells, named chitosan, on the consolidation characteristics of soft soil. At the onset, the material properties of soil and chitosan have been discussed. The latter part of the manuscript details the one-dimensional consolidation tests conducted on soils amended with various chitosan dosages of 0.5%, 1%, 2%, and 4%. The effect of the aforementioned dosages on the coefficient of consolidation, compression index, swelling index, and coefficient of permeability has been discussed along with the mechanism causing the variation. Cracking in soils is a common phenomenon under soil–atmosphere interaction in clayey soils. Additionally, evaporation has a profound influence on the thermo-hydro-mechanical behavior and engineering properties of soils, and hence the potential of untreated and treated soils against shrinkage cracking was evaluated by bar linear shrinkage tests. To assess the contribution of chitosan to greenhouse gas emissions, carbon footprint analysis (CFA) of a typical landfill liner section amended with chitosan has been carried out in the current study.

2. Materials and Methods

2.1. Materials

2.1.1. Soil

Soil excavated from Kuttamangalam, Kuttanad, Kerala, India (9°29′14.9″ N 76°23′25.1″ E) from a depth of 2 m was used for the study. The basic properties of the soil were determined based on relevant ASTM codes. The physical properties of the soil are presented in Table 1, and the particle size distribution is shown in Figure 1.

Table 1. Index and geotechnical properties of studied soil.

Characteristics	Values	Codes Referred
Specific gravity	1.83	ASTM D854-14 [58]
Plastic limit (%)	42.57	ASTM D4318-17e1 [59]
Liquid limit (%)	55.73	
% Sand	8	ASTM D2487 [60]
% Silt	40.5	
% Clay	51.5	
USCS Soil Classification	CH	
MDD (g/cm^3)	1.48	ASTM D698-12 [61]
OMC (%)	23.6	
Organic content (%)	12	AASHTO T 267 [62]

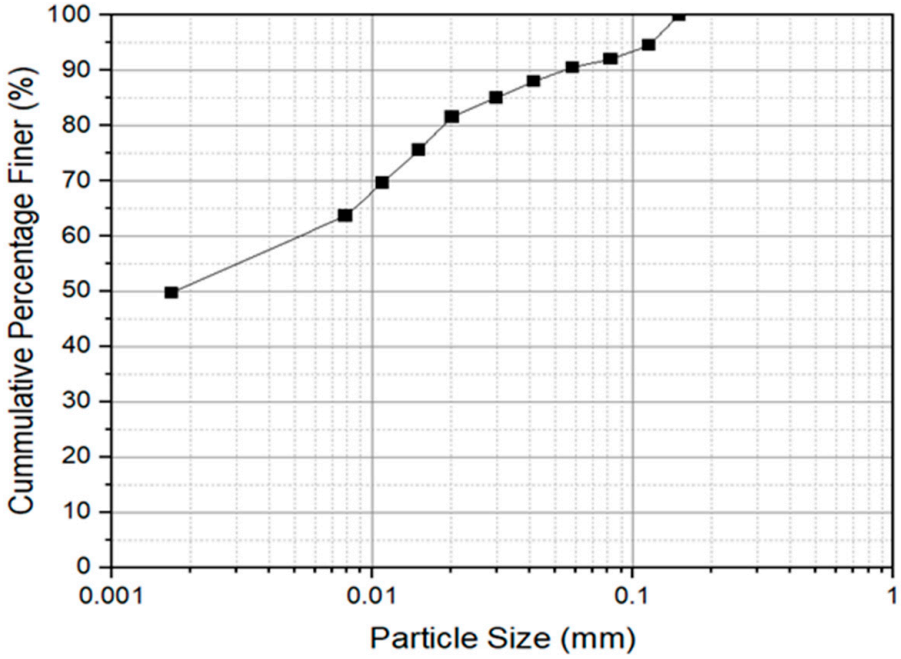

Figure 1. Particle size distribution for the soil.

2.1.2. Biopolymer

Chitosan, an extract from crab or shrimp shells or any other crustacean shells, is the second-most prevalent biological macromolecule after cellulose. It is white in color and flaky in texture. Its nomenclature is 2-acetamido-2-deoxy-α-D-glucose-(N-acetylglucosamine). The chitosan used in the study was purchased from Swakit Biotech Private Limited. It is a flexible, naturally occurring hydrophilic polymer. The polysaccharide chitin, which is present in the exoskeleton of shrimp, lobster, and crabs and the cell mass of numerous parasites, is converted to biopolymer chitosan through N-deacetylation. Chitosan also has applications in the food industry as a thickening agent, manufacturing eco-friendly fertilizers, etc. Chitosan has improved strength by 85% for earthen construction materials [63]. Several studies on soil rejuvenation have confirmed the positive influence of chitosan on the strength characteristics of fine-grained soils [55,64]. It is also proven that the incorporation of chitosan in sandy soils improved the cohesion and other mechanical properties of the soil [54]. The chitosan procured from Swakit Biotech appeared in the form of flakes, with a moisture content and degree of acetylation of 6–8% and greater than 88%. The viscosity is reported in the range of 75–150 csp with a density of 0.25 g/cm^3. The procured soil was treated with various doses of chitosan for the current experimental investigation.

2.2. Methods

2.2.1. Sample Preparation

The soft soil was oven-dried for 24 h and pulverized to fines and the soil passing through a 425 µm sieve was collected for performing the tests. The dry mixing method was adopted for the current study wherein chitosan was added as a percentage of the dry weight of soil. The dosages selected were 0.5%, 1%, 2%, and 4%.

2.2.2. One-Dimensional Consolidation Test

The incremental loading method of a one-dimensional consolidation test was adopted for testing the remolded and chitosan-admixed soil samples in a conventional consolidometer apparatus following ASTM D2435 [65]. The procedure is illustrated in Figure 2. The one-dimensional consolidation test examines the pace and degree of soil settling with lateral confinement and vertical loading. The soil was mixed at an optimum moisture content of 23.6% and the mixture was compacted into consolidation rings of 60 mm diameter and

20 mm height by pressing and kneading to avoid air entrapment. The samples were not subjected to any curing periods for the tests conducted and were immediately subjected to testing. The sample surface was trimmed off to ensure the exact volume of the mold. The ring was placed in the consolidation apparatus and the accessories were fixed thereafter. It was then connected to the outlet with pipe and the sample was arranged for loading. The loading range selected was 12.5–800 kPa and the load increment ratio was fixed as 1. A seating stress of 6.25 kPa was applied initially to ensure the proper seating of the load and the cell alignment. Each load was maintained for approximately 24 h. The coefficient of consolidation was calculated using the logarithm of the time-fitting method using the time-settlement plot. Using the values of the coefficient of consolidation (C_v), the coefficient of volume compressibility (m_v), the unit weight of water (γ_w), and the void ratio (e), the hydraulic conductivity (k) of untreated and amended soils was calculated.

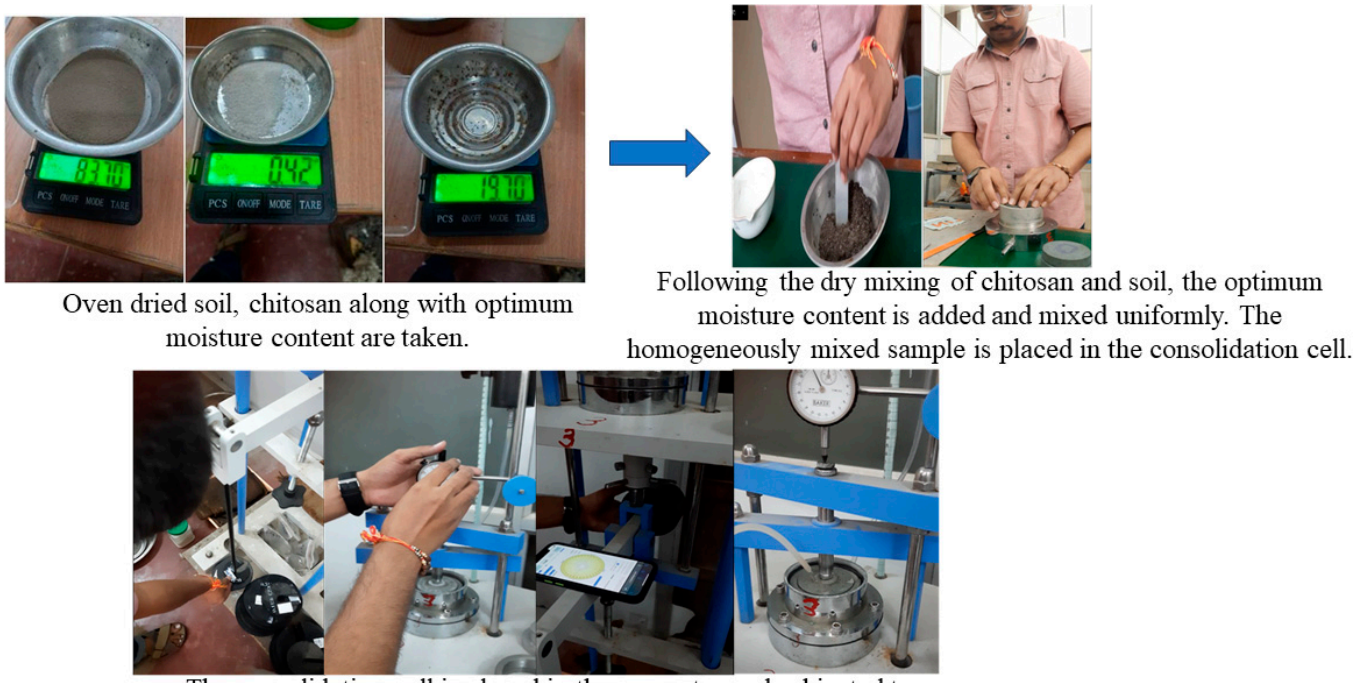

Figure 2. Consolidation procedure undertaken for the study.

2.2.3. Bar Linear Shrinkage Tests

Bar linear shrinkage tests were performed following BS 1377: Part 1-1990 [66] on the chitosan-treated soil. The adopted water content was equivalent to the liquid limit of the chitosan–soil mix for performing the shrinkage tests. A brass mold (141 mm × 20 mm × 12.5 mm) was fabricated for placing the chitosan–soil mix. Free shrinking was allowed by applying a thin layer of silicon grease to the inner sides of the mold. Air pockets were removed by tapping the mold and the mix was leveled along the top of the mold. Air drying of the specimen was allowed until the specimen shrunk and deformed away from the walls of the mold. Natural shrinkage was simulated by exposing the specimen to an atmospheric temperature. A high-resolution camera was fixed from a height to capture the shrinkage process at regular intervals. The tests were conducted twice for the repeatability of results. Equation (1) can be used for computing the linear shrinkage.

$$Linear\ Shrinkage = \left[1 - \frac{L_d}{L_i}\right] \times 100 \quad (1)$$

where L_i = initial length of specimen (mm) and L_d = dried length of specimen (mm).

2.2.4. Scanning Electron Microscopy

The microstructures of soft soil amended with chitosan were studied using a scanning electron microscope (SEM). The air-dried samples were analyzed utilizing TESCAN VEGA 3 LMU high-performance, Variable Pressure Analytical SEM with LAB6 having a high resolution of 2 nm.

2.2.5. Carbon Footprint Analysis (CFA)

The various stages involved in a material or service, such as its production, transportation, and field application, directly or indirectly release various gases into the environment, which may have an impact on the global warming crisis. The extent of the impact of these gases is defined by the term "Carbon Footprint". The global mean temperatures are on the rise due to the increased concentration of CO_2 in the atmosphere over the years. The consideration of all the gases in analyzing the carbon footprint of a project is a comprehensive procedure. A parameter called CO_2 equivalent was introduced by [67,68] to convert the effect of each gas into a single unit for easier comparison and analysis. The equivalent unit of CO_2 is named as embodied carbon equivalent factor (ECF). The current study utilized the normalized ECFs to calculate the carbon emissions released throughout the different phases.

The carbon emission analysis is divided into 3 phases:

1. Consideration of materials required for the project.
2. Acquisition and haulage of materials.
3. Site operations in the project site.

3. Results

3.1. Effect of Chitosan on Compression Index (C_c) and Swelling Index (C_s)

Consolidation experiments demonstrated the soil–biopolymer mix's compressibility in the presence of water. The changes in void ratio with varying consolidation pressures for different chitosan dosages are displayed in Figure 3. The volume change occurring within the untreated soil matrix during the loading stage is primarily due to the slipping of the particles. These particles do not regain their original positions upon the removal of the load increment. The marginal rebound occurring upon unloading is due to the elastic compression of the adsorbed water around the particles and is a peculiarity of kaolinite-rich soils [69]. The compressibility curves of the chitosan-treated soils took a downward shift compared to the untreated soil. This indicates that the void ratio of the treated soils reduced considerably from 1.0 to 0.3 up to a dosage of 2%. The final equilibrium void ratio for the treated soils up to a 2% dosage has been reduced for the loading duration compared to untreated soil. For all dosages, it can be noted that the void ratio change is marginal at lower consolidation pressure of 25 kPa. The lower pressure is insufficient to cause pore water expulsion, leading to minimal volume change in the untreated and treated soils. The compressibility achieved can be due to the shearing resistance at the near contact points and the change in the volume of the soil sample as a result of shear displacement [70]. However, the 4% dosage led to an increase in void ratio as exhibited in Figure 3. Chitosan can act as a flocculating agent, causing soil particles to aggregate and form larger particles. This can reduce the overall surface area of the soil and decrease the void ratio. The higher strength and stiffness imparted by the flocculation phenomena lead to an increased resistance against compression [71]. At higher dosages of 4%, there is the formation of clumps, which occupy the soil matrix and lead to an increase in voids, which aids in the removal of pore water upon application of surcharge loads.

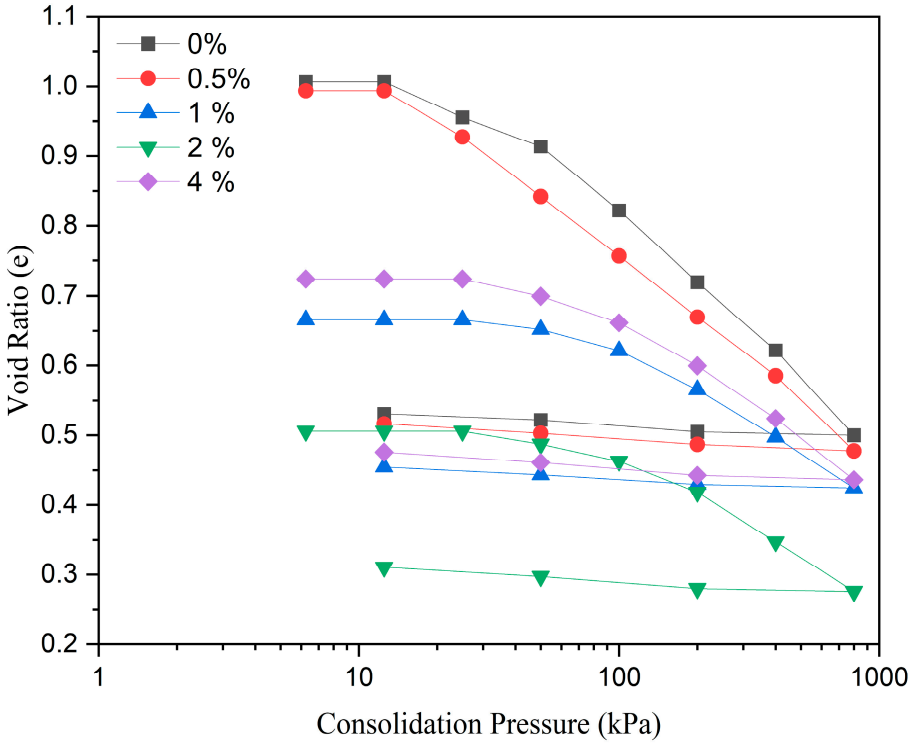

Figure 3. Effect of chitosan inclusion on the volume change behavior.

The trend observed for the compression index and swelling index of the soil upon interaction with chitosan particles has been discussed (Figures 4 and 5). The compressibility index (C_c) denotes the change in void ratio with regard to the rise in effective stress. Upon an increase in pressure, electrostatic forces that hold water are not sufficient and lead to the expulsion of water [34]. The compressibility of the soil increased with a rise in consolidation pressure for the untreated and amended soils due to a decrease in soil thickness. Under the influence of lower loads for 0.5%, the increase in the diffused double layer of the soil increases its thickness, leading to a drop in C_c, especially at 25 kPa and 50 kPa. This positive modification in C_c is more beneficial than the xanthan-gum-treated kaolinite wherein the compressibility further increased at the same dosage of 0.5% [72–74]. The modification in C_c due to different biopolymers on kaolinite is presented in Table 2. The situation can be further aggravated in kaolinite in the presence of organic content. The high water-holding capacity of the organic matter and xanthan gum will further elevate the porosity of the xanthan gum–soil mix, leading to higher compressibility [75]. Hence, the detrimental effect of xanthan gum on organic soils can be mitigated by the inclusion of polysaccharide biopolymers as indicated in the present study. The C_c value continued to drop with an increase in chitosan dosage compared to unamended soil. A marginal increase in C_c was observed beyond 2%, owing to the agglomeration of particles into clumps and eventually decreasing the void ratio. This can be attributed to soil grain binding via hydrogen bonding between the OH group of chitosan and the positively charged edges of clay particles [76]. Generally, the untreated soil exhibited negligible rebound upon unloading (load decrement ratio of 4). The same trend was exhibited by the soil treated with different dosages of chitosan. The swelling index (C_s) decreased from 0.015 for untreated to 0.007 for the 2% dosage, beyond which the swelling index slightly increased to 0.011 for 4% at 200 kPa. At lower stresses of 12.5 kPa and 50 kPa, the swelling indices initially dropped with an increase in chitosan dosage and rose to a maximum at 4% dosage. The reduced swell values of the treated soils indicate that chitosan addition subdues the swelling capacity of the soil, which can be beneficial during and after construction. The reduction in the compressibility and swelling of kaolinitic soils using chitosan is higher than that of xanthan-gum-treated kaolinite [46].

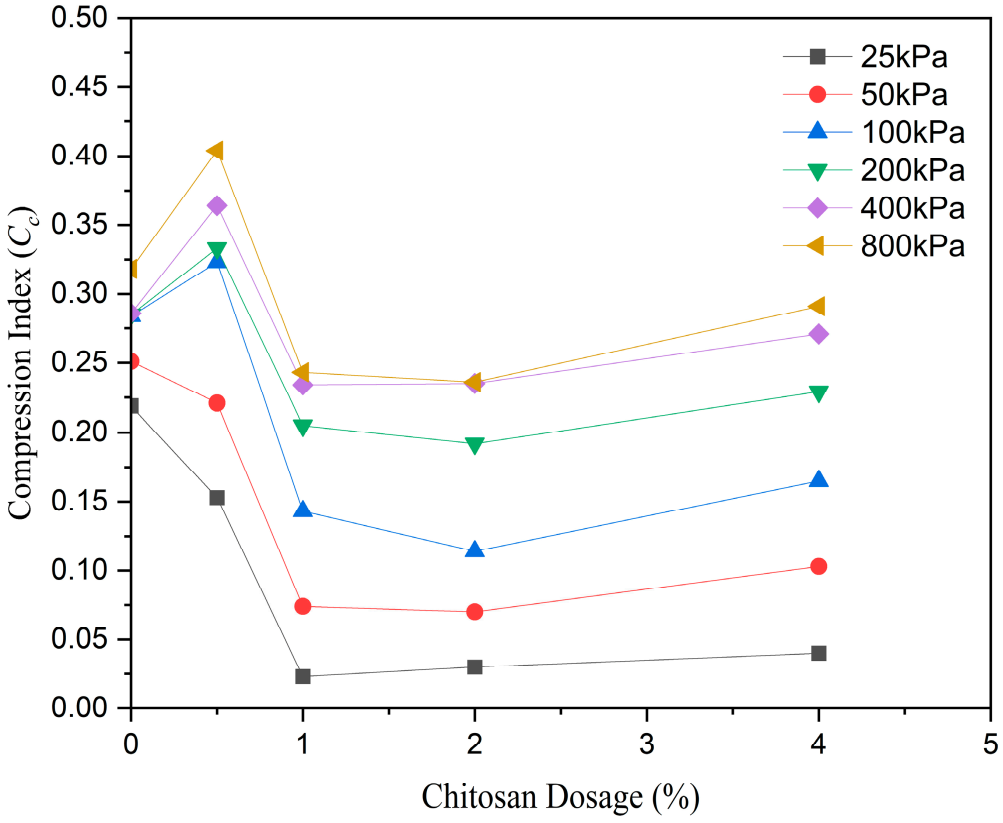

Figure 4. Variation in compression index with an increase in dosage of chitosan.

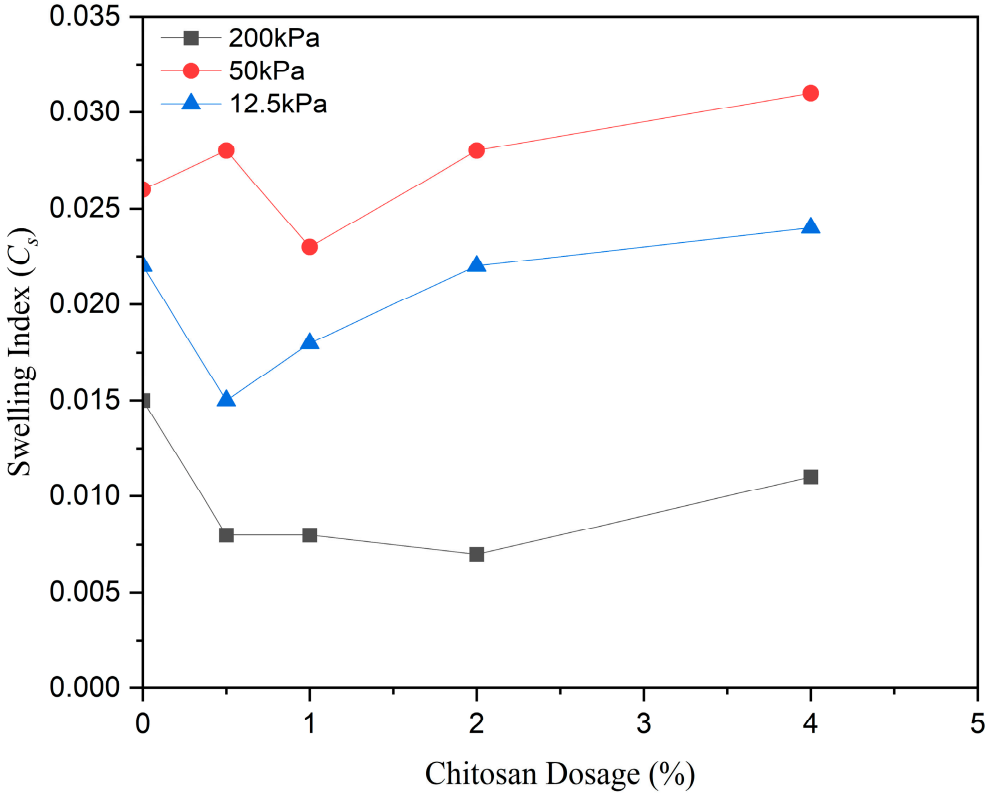

Figure 5. Variation in swelling index with an increase in dosage of chitosan.

Table 2. Effect of different biopolymers on the compressibility index of kaolinite soils.

Biopolymer Type and Dosage	Compression Index, C_c		Reference
	Untreated	Treated	
Chitosan; 0.5%	0.284	0.170	Current study
Xanthan Gum; 0.5%	0.030	0.170	[72]
Xanthan Gum; 0.5%	0.387	0.405	[73]
Xanthan Gum; 1%	0.160	0.190	[74]

3.2. Effect of Chitosan on Coefficient of Consolidation (C_v) and Hydraulic Conductivity (k)

The coefficient of consolidation (Figure 6) and hydraulic conductivity (Figure 7) were calculated for every dosage of chitosan. The C_v values for untreated soil decreased as the pressure increased from 100 to 800 kPa owing to pore water ejection, which affected the soil structure and resulted in a decrease in the void ratio. At 100 kPa, the untreated soil possessed a coefficient of consolidation of 6.24 m^2/year, which increased with an increase in the dosage of chitosan, i.e., 10.08 m^2/year for 0.5%, 19.28 m^2/year for 1%, and a maximum value of 43.32 m^2/year for 2%, which is nearly seven times that of untreated soil, and then decreased again to a value of 10.74 m^2/year for the 4% chitosan dosage. This indicates that the addition of chitosan accelerated the consolidation process up to a dosage of 2% in a shorter duration and then decelerated. A similar increase in C_v has been reported for low organic soil treated with nano calcium carbonate [76]. However, the rate of increase in C_v is lower compared to chitosan-amended soil. The non-cohesiveness of chitosan promoted an easy expulsion of free water [57]. At all dosages, the C_v values were higher than that of untreated soil.

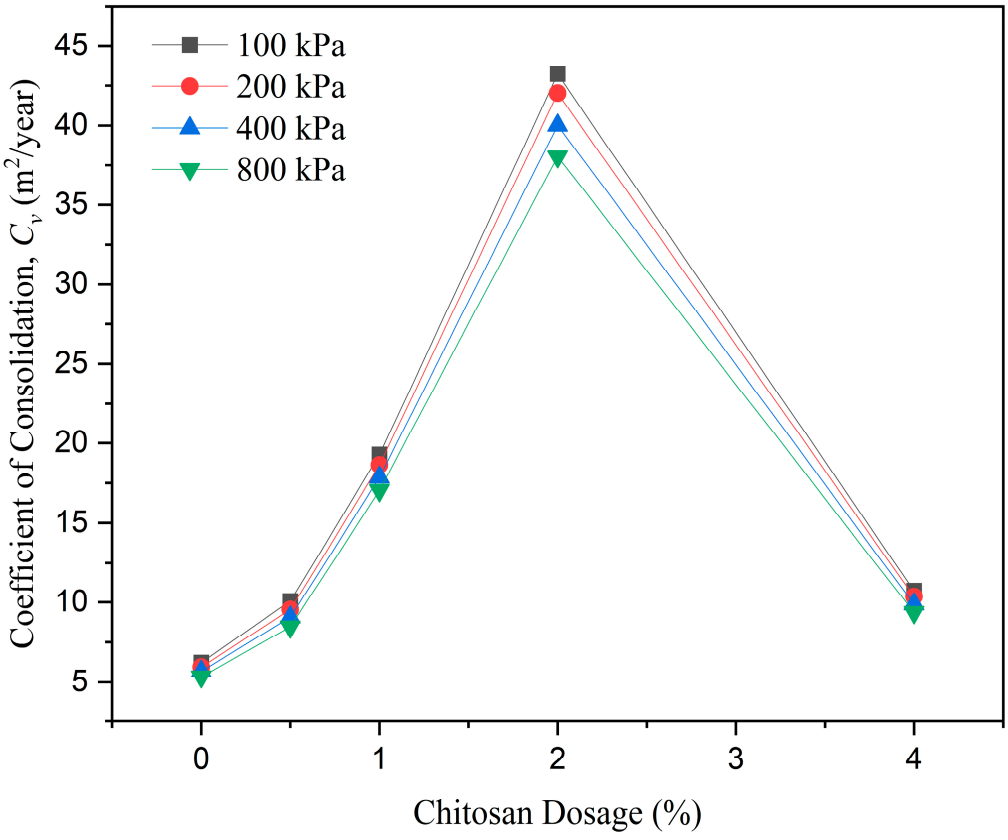

Figure 6. Variation in coefficient of consolidation with an increase in dosage of chitosan.

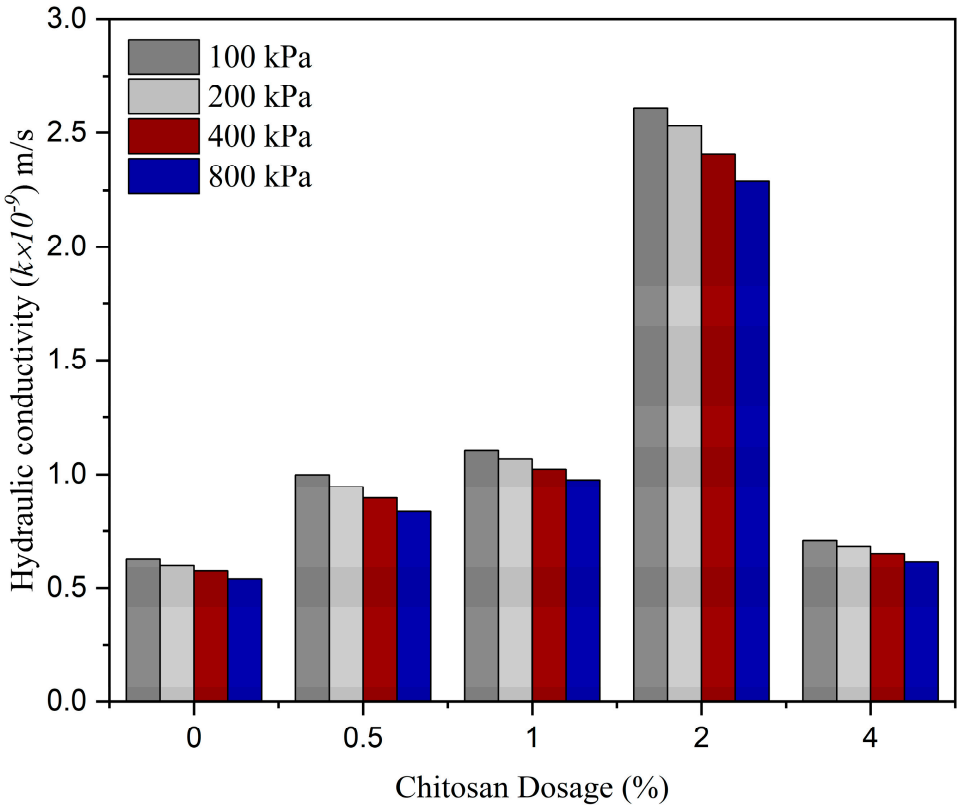

Figure 7. Variation in hydraulic conductivity with an increase in dosage of chitosan.

The addition of chitosan in the soil causes the aggregation of soil particles by being a lightweight and voluminous filler material as depicted in Figures 8 and 9. This mechanism results in a reduction in the number of contact points and thus increases the flow path for the pore water expulsion. This leads to a marginal increase in hydraulic conductivity value (k) upon 0.5% of chitosan inclusion within the soil matrix at 100 kPa. With an increase in consolidation pressure, there was more expulsion of water, resulting in a reduced void ratio and hydraulic conductivity. This trend was observed for untreated and chitosan-amended soils. At 1% and 2%, the hydraulic conductivity increased by 1.74 times and 4.14 times compared to untreated soil. The increase in hydraulic conductivity in such low organic soils during the earlier curing period has been observed after amendment with nano calcium carbonate [76]. Nano calcium carbonate and chitosan serve as fillers within the matrix of organic soils, leading to the agglomeration of particles. Dosages beyond 2% lead to a drop in the void spaces and hydraulic conductivity of the chitosan–soil matrix. The addition of a dosage beyond the optimum facilitates cluster formations between soil lumps causing the blockage of the flow path. The blockage created within the structure resulted in a decrease in the rate of pore water expulsion, causing a dip in the coefficient of consolidation and hydraulic conductivity for the 4% dosage. Another factor responsible for the reduction in the value of the coefficient of consolidation is the hydrophilic nature of the chitosan, which holds the pore water and does not allow it to expel out, leading to decreased k values.

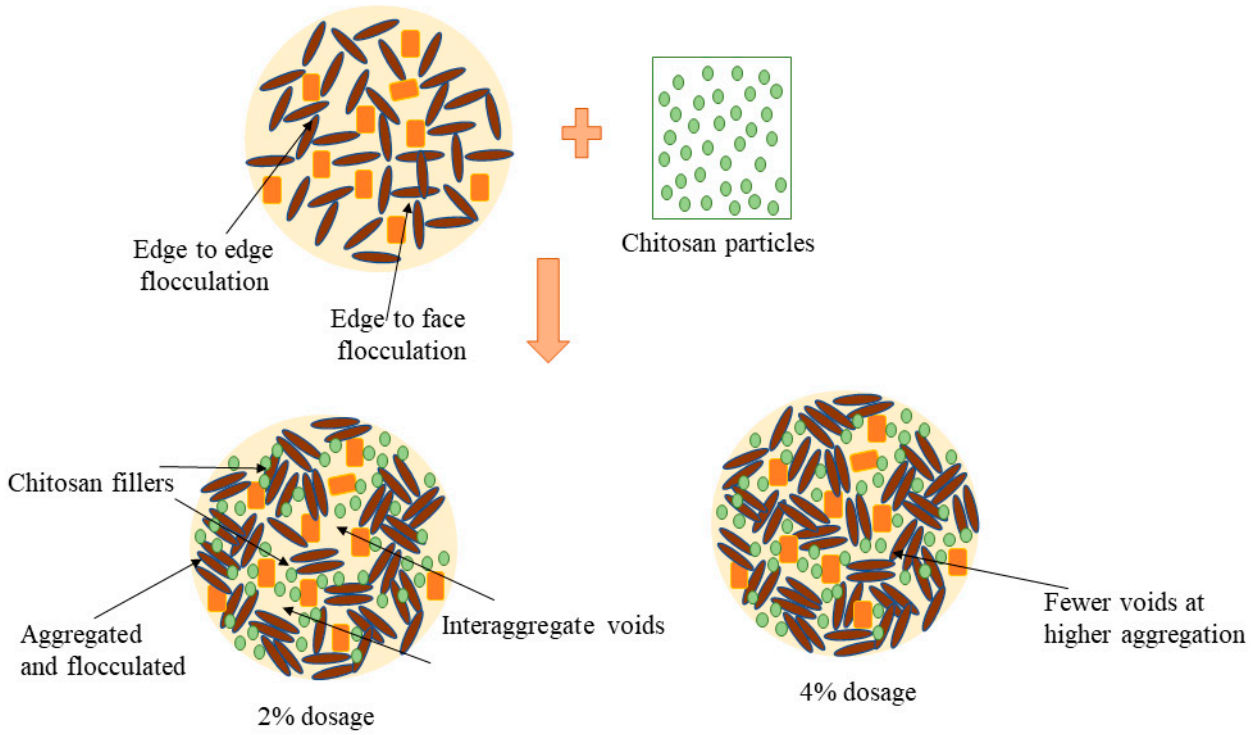

Figure 8. Bridging mechanism of chitosan-treated soft soil.

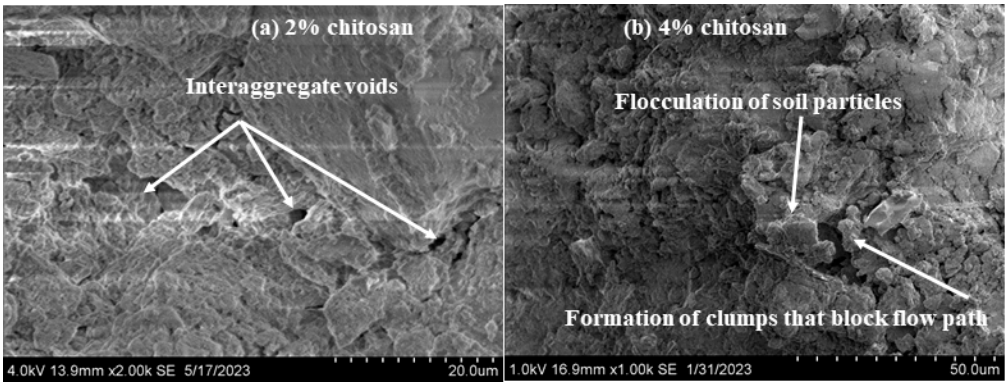

Figure 9. SEM images of chitosan-amended soils treated with (**a**) 2% dosage and (**b**) 4% dosage.

3.3. Shrinkage Phenomena in Chitosan-Soil Mix

The samples for the different dosages were prepared at the liquid limit. The liquid limit was conducted as per ASTM D4318-17e1 [59]. The values of liquid limits were estimated as 55.73%, 58.50%, 64.64%, 68.85%, and 68.82% for 0%, 0.5%, 1%, 2%, and 4% of chitosan. The addition of chitosan leads to the modification of the electrical double layer and specific area of kaolinite by creating interparticle voids. This phenomenon increases the volume of water held in the soil matrix, leading to an increase in the liquid limit [56]. The soil prepared for shrinkage tests were subjected to drying by exposing to natural conditions, leading to a volume change. The performance of soil during the shrinkage process can be evaluated by considering the change in length, amount of lift, or surface characteristics, such as the curling or cracking of the samples [77]. The linear shrinkage for the untreated soil is estimated to be 14.18%. The reduction in moisture content led to a reduction in height and detachment of the sample from the sides of the mold. The test setup for observing the shrinkage phenomena is presented in Figure 10.

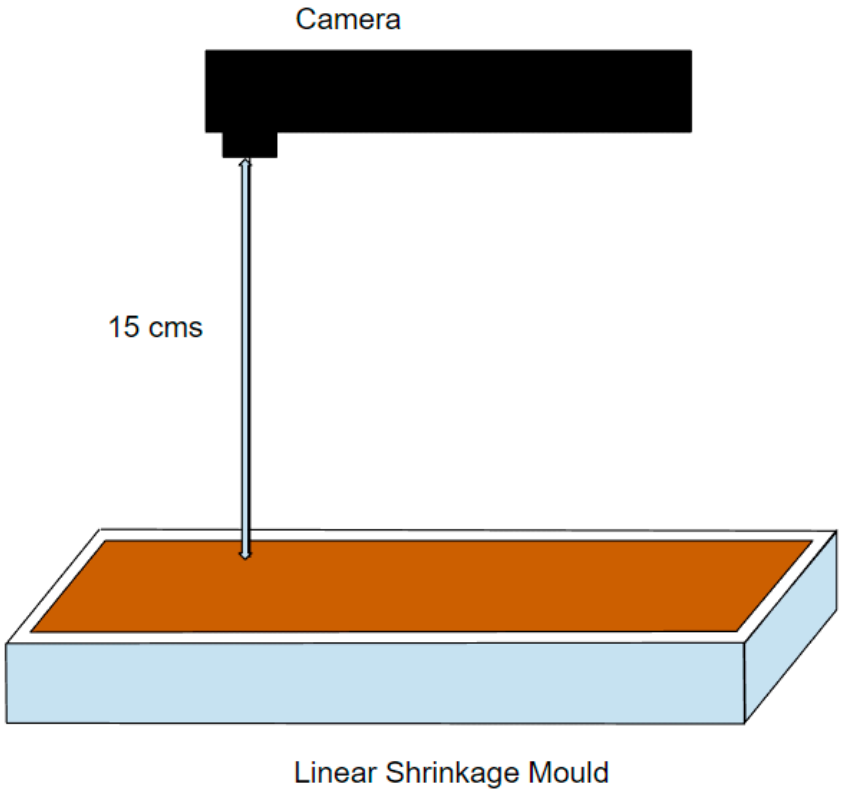

Figure 10. Linear shrinkage test setup.

Figure 11 displays the shrinkage phenomena captured for the untreated and chitosan-treated samples. The treatment with chitosan led to a reduction in the linear shrinkage of the soil samples as indicated in Table 3. Following the detachment from the mold, the samples started to shrink in all directions. The deformation was higher in the longitudinal direction for all the treated samples. The lowest shrinkage was noted for the highest dosage (4%) adopted for the study. The untreated and treated samples did not exhibit any curling or cracking during the process of shrinkage.

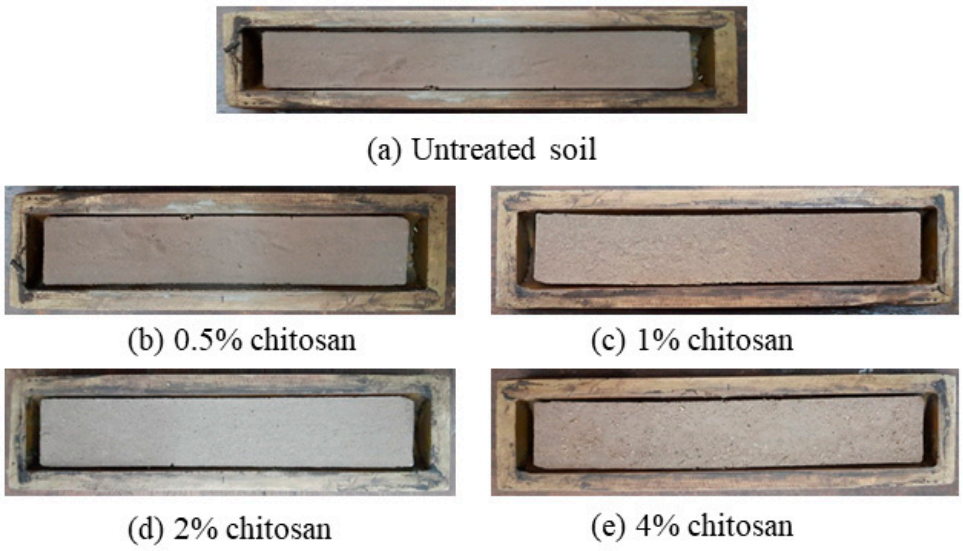

Figure 11. Shrinkage of studied soil (**a**) untreated and soil treated with chitosan dosages of (**b**) 0.5% (**c**) 1% (**d**) 2% (**e**) 4%.

Table 3. Linear shrinkage of chitosan–soil mixes.

Description	Final Length at the End of Drying (mm)	Percentage of Linear Shrinkage (%)
Untreated Soil	128.73	14.18
Soil + 0.5% Chitosan	129.01	13.99
Soil + 1% Chitosan	130.49	13.01
Soil + 2% Chitosan	130.9	12.73
Soil + 4% Chitosan	131.15	12.57

3.4. Environmental Impact of Chitosan

The environmental impact of a material has to be assessed from cradle to grave. Due to the escalating global warming crisis, it is important to ascertain the contribution of any civil engineering material or work to climate change issues. Since its inception, any material plays an important role in the release of greenhouse gases. In this regard, chitosan has been resourced from marine waste, ensuring its recyclability. Previous studies have proved that chitosan's contribution to the carbon footprint is much lesser than traditional chemical materials such as cement and lime [71]. Contrary to the detrimental effects on flora and fauna by chemical stabilizers, chitosan has been shown to promote vegetation effectively and sustain microbial life within the soil [78,79]. Chitosan can thus be a promising alternative to chemical stabilizers for soft soil amelioration from a geotechnical and environmental point of view.

3.5. Recommended Application from the Results

The hydraulic conductivity of the liner is a significant parameter in the selection of liner material. Due to the non-availability of low permeable soils, soil amendment becomes imperative for achieving the desired properties of a liner. The performance of a liner requires the assessment of the hydro-mechanical behavior of a material [80]. The current study evaluated the efficacy of a polysaccharide biopolymer named chitosan in addressing the compressibility and desiccation cracking of amended clayey soil. Chitosan-amended soils have modified the soil fabric to achieve reduced values of hydraulic conductivity [81]. The hydraulic conductivity of the soil obtained at a 4% dosage is much less than that required for a landfill liner (10^{-7} cm/s) [82]. At all dosages, the hydraulic conductivity satisfied the minimum criteria to be fulfilled by the landfill liner. The evaporation of water in soil upon drying leads to volumetric shrinkage and differential movement, resulting in structural damage. In landfills, desiccation cracking will lead to the leakage of landfill liners and affect the integrity of the liner system. The promising results obtained from the shrinkage study revealed that desiccation cracking can be effectively controlled by the inclusion of chitosan. Thus, chitosan-amended soft soil can be recommended as a landfill liner.

3.6. Carbon Emissions Resulting from the Construction of a Landfill

A landfill is considered for the study to serve a community of one lakh population for a design period of 50 years. As shown in Figure 12, the landfill has a width of 600 m with a side slope of 1.5:1 below the ground level and 3:1 above the ground level. The compacted clay liner (CCL) at the base with a thickness of 1 m is provided and the liner in the soil cover is provided with 0.5 m thickness. From the preliminary results of the study, the soil was compacted to a uniform density of 1.48 g/cm^3 (or t/m^3), and a moisture content of 23.6% was added with a 2% dosage of chitosan.

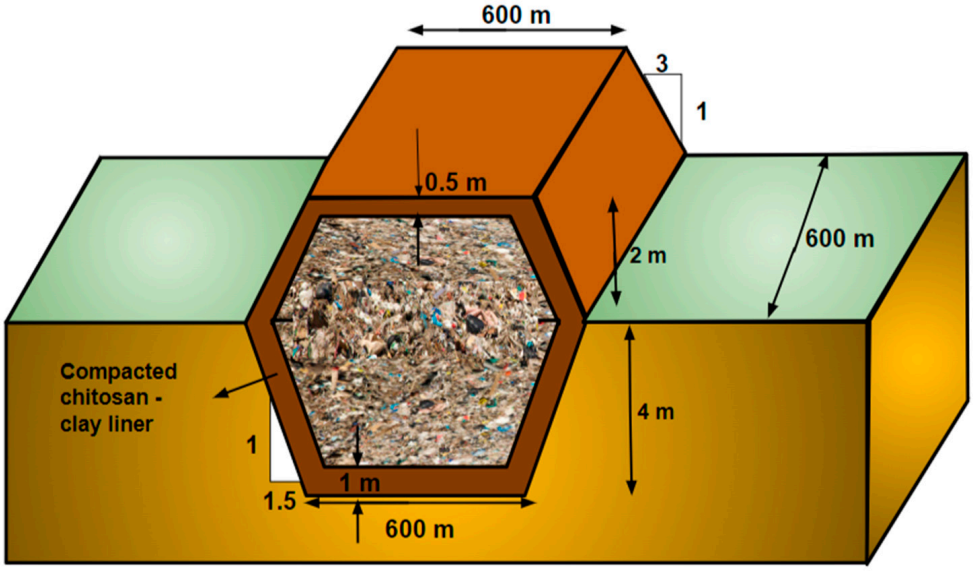

Figure 12. Schematic diagram of landfill with CCL treated with chitosan.

3.6.1. Phase 1: Calculating Embodied Carbon Emissions from the Materials

The materials considered for the analysis included soil, chitosan, and the required quantity of water. The ECF values of these materials were taken from [67,68,83–85] to indicate the embodied carbon emissions. The dimensions of the landfill were fixed based on the general design guidelines. Based on the dimensions, the volume of soil required for the construction of the landfill liner components was estimated. The weight of chitosan and water was estimated as a percentage of the total weight of the estimated soil quantity. The weights multiplied by the respective ECF values determined the carbon emissions contributed by soil, chitosan, and water. Table 4 displays the values of Phase 1 carbon emissions. The calculations are presented in Appendix A.

Table 4. Embodied carbon emissions from Phase 1.

Phase 1	Materials	Amount (m^3)	Unit Weight (t/m^3)	Weight (t)	ECF	CO_2e (t)
Embodied carbon of the material	Clay	5,41,615.73	1.48	801,591.28	0.0056	4488.91
	Chitosan	64,127.32	0.25	16,031.83	0.0074	118.64
	Water	1,89,175.54	1	189,175.54	0.0010	189.18
Total CO_2e (t) Emission in Phase 1.						**4796.73**

3.6.2. Phase 2: Calculating Embodied Carbon Emissions Resulting from Acquisition and Haulage of Materials

The second phase involves the quantification of carbon emissions from the material's acquisition and delivery to the site. The machines considered were a heavy-duty dumper with a 25 t/L capacity for hauling and a pickup excavator with a 10 t/L capacity for procurement. To make quantification easier, the to and fro haulage distance was set at 1 km. The gasoline needed for these cars, which was derived from [84,86,87], had its ECF values taken into account. The values of the embodied carbon emissions caused by the material's acquisition and transportation are shown in Table 5. The hauling distance, vehicle capacities, and fuel types utilized by the vehicles had a significant impact on the emissions from this phase.

Table 5. Embodied carbon emissions from Phase 2.

Phase 2	Process	Vehicle	Capacity (t)/L	Trips	Total Fuel (L)	ECF	CO_2e (t)
Excavation and loading	Clay Procurement	Pickup Excavator	10	80,159	80,159	3.25	260,516.75
	Chitosan Procurement	Pickup Excavator	10	1604	1604	3.25	5213.00
Total CO_2 e(t) emission in the excavation and loading phase							265,729.75
Phase 2	**Process**	**Vehicle**	**Capacity (t)/L**	**Trips**	**Total Fuel (L)**	**ECF**	**CO_2 e (t)**
Haulage	Clay Haulage	Heavy-Duty Dumper	25	16,032	16,032	3.25	52,104.00
	Chitosan Haulage	Heavy-Duty Dumper	25	321	321	3.25	1043.25
Total CO_2 e(t) emission in the haulage phase							53,147.25
Total CO_2e (t) emission in Phase 2							**318,877.00**

Note: Total fuel is calculated for half a trip of a unit distance.

3.6.3. Phase 3: Calculating Embodied Carbon Emissions of the Site Operations

The site operations contributing to the carbon emissions were considered and analyzed in Phase 3. A bulldozer with a 10 t/L capacity for spreading soil, a slurry mixer with a 0.5-t capacity for mixing chitosan, a distributor truck with a 7000 L capacity for spraying chitosan, a sheep foot roller with a 12 t/L capacity for compacting soil in the baseliner, a smooth wheel roller with a 12 t/L capacity for compacting the final cover, and a slope compactor roller with a 9 t/L capacity for compacting soil in the side liner were considered in the analysis. Table 6 presents the carbon emissions evaluated during Phase 3. The vehicle capacities and the number of trips affected the total carbon emissions in Phase 3, similar to Phase 2. The calculations and total carbon emissions from all three phases are reported in Appendix A and Table 7, respectively.

Table 6. Embodied carbon emissions from Phase 3.

Phase 3	Process	Vehicle	Capacity	Trips	Total Fuel (L)	ECF	CO_2e (t)
Site operation	Spreading	Bulldozer	10 t/L	81,763	81,763	3.25	265,729.75
	Spraying of chitosan	Distributor truck	7000 L	30	30	3.25	97.50
	Compaction	Sheep foot roller	12 t/L	30,000	30,000	3.25	97,500.00
		Slope compactor roller for slopes below ground level	9 t/L	962	962	3.25	3126.50
		Slope compactor roller for slopes above ground level for cover	9 t/L	419	419	3.25	1371.75
		Smooth wheel roller for the final cover	12 t/L	15,000	15,000	3.25	48,750.00
Total CO_2e (t) emission in Phase 3							**4,16,575.25**

Table 7. Total embodied carbon emissions from the three phases considered.

Phase	Operation	Embodied Carbon CO_2e (t)
Phase 1	Materials	4796.73
Phase 2	Procurement and Haulage	318,877.00
Phase 3	Site Operations	416,575.25
Total CO_2e (t) emissions from all three phases		**740,248.98**

3.6.4. Comparison of Carbon Emissions of Chitosan with Traditional Stabilizers

With optimal dosages of 4% and 6%, respectively, the carbon emissions for the planned landfill with cement and lime employed as amendments were studied; these emissions are presented in Table 8 [88,89]. Phase 1 alone was considered to make a direct comparison. Only Phase 1 was taken into consideration for the comparison to consider the impact of the various materials. Phases 2 and 3 were omitted for comparison because of the influencing factors, such as the vehicle capacity, fuel type, and haulage distance. As indicated in Figure 13, the carbon emissions with 4% cement and 6% lime contributed 45.376% and 54.451% of the total emissions, respectively, whereas chitosan provided 0.173%. The ECF values of lime and cement were found to be 0.76 and 0.95, respectively [67,68].

Table 8. Embodied carbon emission comparison of chitosan with lime and cement.

Materials	Dosage (%)	Quantity Required (t)	ECF	CO_2e (t) (Stabilizer)	CO_2e (t) (Clay)	CO_2e (t) (Water)	CO_2e (t) Emission in Phase 1
Chitosan	2	16,031.83	0.0074	118.64	4488.91	189.18	4796.73
Lime	6	49,095.48	0.76	37,312.57	4488.91	189.18	41,990.66
Cement	4	32,063.65	0.95	30,460.47	4488.91	189.18	35,138.56

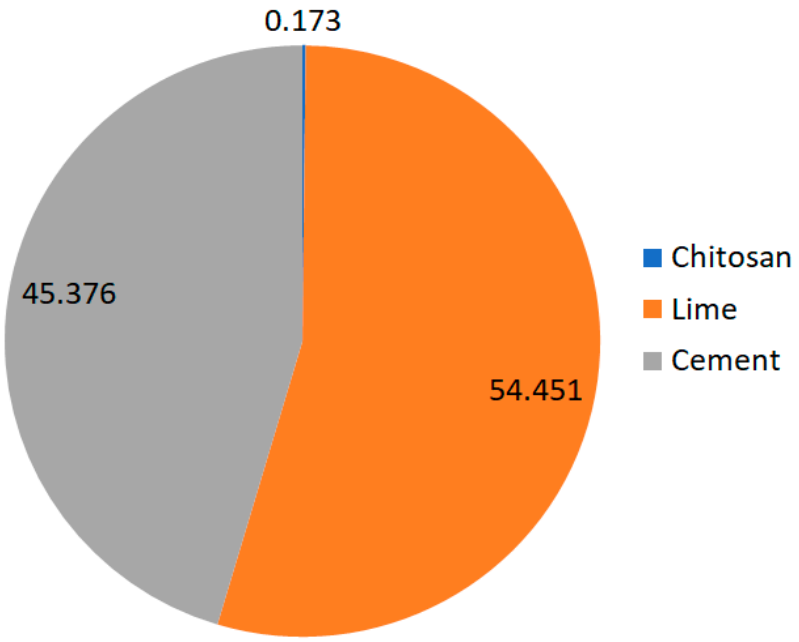

Figure 13. Comparison of carbon emission of chitosan with lime and cement.

4. Conclusions

The utilization of marine waste in enhancing the engineering properties of soft soil deposits is gaining popularity as it addresses the issue of waste management and disposal and negates harmful effects on the environment. The following conclusions are drawn from the study, which evaluated the consolidation characteristics, shrinkage phenomenon, and sustainability factor of chitosan-treated soft soil:

- The role of chitosan as a flocculating agent caused the flocculation of soil particles and reduced the overall surface area of the soil, and decreased the void ratio by 70% up to an optimum of 2%. The untreated and treated soils exhibited negligible swelling upon unloading at a load decrement ratio of 4.
- The addition of chitosan quickened the consolidation process by allowing for easy pore water expulsion by seven times compared to untreated soil up to a 2% dosage, owing to its non-cohesive nature.

- With a dosage more than the optimum, flow paths are blocked due to the formation of clusters aggravated by the presence of chitosan fillers, thus resulting in a decrease in pore water expulsion that, in turn, decreased the value of the coefficient of consolidation and hydraulic conductivity
- The inclusion of chitosan in soil showed tremendous improvement in the reduction in shrinkage. The untreated and treated samples did not exhibit desiccation cracking and a maximum reduction in shrinkage by 11% was achieved with a 4% dosage.
- The CFA carried out for a typical landfill liner revealed that the addition of chitosan to the studied soil can reduce the associated carbon emissions by 8.754 and 7.325 times compared to traditional stabilizers like lime and cement, respectively.

The amelioration of soft soil with chitosan is a promising alternative to other chemical stabilizers and biopolymers as it accelerates the consolidation process in addition to being environmentally friendly. Additionally, chitosan has proven its efficacy in controlling desiccation cracking. The sustainability assessment of chitosan-amended soft soil revealed that the carbon footprint can be significantly reduced and can easily replace the other stabilizers employed in ground improvement works. The only limitation is the high cost of chitosan (1300 Rs/kg), which can be solved by expanding the market through widespread implementation. One of the main reasons for the increased rate of chitosan is due to limited application in the geotechnical engineering field compared to other fields such as medicine, cosmetics, and the food industry. Due to the promising results observed in the current study, this amendment can be applied to liner systems built in any geoenvironmental application involving soft soil.

Author Contributions: Conceptualization, methodology, R.M.R., S.S.R.J. and A.A.B.M.; formal analysis, investigation, R.M.R.; resources, A.A.B.M.; data curation, R.M.R., S.S.R.J. and A.A.B.M.; writing—original draft preparation, R.M.R., S.S.R.J. and A.A.B.M.; writing—review and editing, R.M.R., S.S.R.J., A.A.B.M., A.U.R. and B.C.S.C.; visualization, A.A.B.M.; supervision, A.A.B.M.; project administration, A.A.B.M.; funding acquisition, A.U.R. All authors have read and agreed to the published version of the manuscript.

Funding: This research was funded by King Saud University through Researchers Supporting Project number (RSPD2023R701), King Saud University, Riyadh, Saudi Arabia.

Data Availability Statement: All data used during the study appear in the published article.

Acknowledgments: The authors are thankful to King Saud University for funding this work through the Researchers Supporting Project number (RSPD2023R701), King Saud University, Riyadh, Saudi Arabia.

Conflicts of Interest: The authors declare no conflict of interest.

Appendix A

A landfill was considered for the study to serve a community of one lakh population for a design period of 50 years. Assuming that there is an increase in population in an arithmetic manner with an increase of ten thousand per decade, as per indieeducation.com, the amount of waste generated on average by a person per day in India is 0.45 kg.

Population at the end of 50 years	100,000 + 10,000 × 5 150,000
Amount of waste generated (Factor of safety adopted = 1.5)	150,000 × 0.45 × 1.5 × 365 × 50 1,847,812,500 kg
Assuming that the waste is compacted to the maximum possible density, i.e., 961 kg/m^3 [90].	
Volume of the waste	1,847,812,500/961 1,922,801.77 m^3
The following landfill dimensions were considered:	
Base width	600 m
Side slopes	1:5:1
Depth	4 m
Slope of the final cover	3:1
Width of the final cover	600 m
Length of landfill	600 m
Check: The volume that can be accommodated with the given dimensions is [0.5 × 4 × (600 + 612) + 0.5 × 2 × (612 + 600)] × 600 = 2,181,600 m^3 (>1,922,801.77 m^3).	
Thickness of the CCL base liner	1 m
Thickness of the liner in the final cover	0.5 m
Dosages and properties of material considered:	
Required density	1.48 t/m^3
Water content	23.6%
Chitosan	2%
Volume of clay liner and quantity of materials calculated from the given data:	
Volume of CCL required for the baseliner	[1 × 600 + 1 × 2 × ($\sqrt{}$42 + (4 × 1.5) × 2)] × 600 1 × 600 + 2 × 7.211 × 1] × 600 368,653.32 m^3
Volume of CCL required for the final cover	[0.5 × 600 + 0.5 × 2 × $\sqrt{}$(22 + (3 × 2) × 2)] × 600 183,794.73 m^3
Total quantity of CCL required	552,448.05 m^3
Total quantity of soil	Density × Volume 1.48 × 552,448.05 m^3 817,623.11 t
Let the weight of clay required be 'x'; then, the weight of chitosan required is equal to '0.02 × x'. Therefore, the total weight of the soil is equal to 1.02 × x. Equating both the expressions, we obtain 1.02 × x = 817,623.11 t	
Clay	817,623.11/1.02 801,591.28 t
Chitosan	0.02 × 801,591.28 t 16,031.83 t
Water	0.236 × 801,591.28 t 189,175.54 t

Embodied carbon emissions from Phase 1 (Materials).

CO_2e from Material	**ECF of Material × Quantity**
CO_2e from Clay	0.0056 × 801,591.28 4488.91 t
CO_2e from Chitosan	0.0074 × 16,031.83 118.64 t
CO_2e from Water	0.0010 × 189,175.54 189.18 t
Total CO_2e from Phase 1	**4796.73 t**

Embodied carbon emissions from Phase 2 (Procurement and Haulage).

A pickup excavator of 10 t/L capacity for procurement and a heavy-duty dumper of 25 t/L capacity for haulage were considered. The haulage distance was considered to be 1 km (to and fro) for easy quantification.

Total Fuel for Procurement	Quantity/(Capacity of Vehicle)
Total fuel for haulage	(0.5 × Quantity)/(Capacity of a vehicle)
CO_2e from fuel	ECF of fuel × Total fuel
Procurement of clay:	
Total fuel	801,591.28/10
	80,159 L
CO_2e emitted	3.25 × 80,159
	260,516.75 t
Procurement of chitosan:	
Total fuel	16,031.83/10
	1604 L
CO_2e emitted	3.25 × 1604
	5213.00 t
Haulage of clay:	
Total fuel	0.5 × (801,591.28/25)
	16,032 L
CO_2e emitted	3.25 × 16,032
	52,104 t
Haulage of chitosan:	
Total fuel	0.5 × (16,031.83/25)
	321 L
CO_2e emitted	3.25 × 321
	1043.25 t
Total CO_2e emitted from Phase 2	**318,877.00 t**

Embodied carbon emissions from Phase 3 (Site operations).

A bulldozer of 10 t/L capacity for spreading soil, a distributor truck of 7000 L capacity for spraying chitosan, a sheep foot roller of 12 t/L capacity for compaction of the base liner, a slope compactor roller of 9 t/L capacity for compaction of side slopes both above and below ground level, and a smooth wheel roller of 12 t/L capacity for compaction of soil on the final cover were considered.

Spreading of Soil (Bulldozer)	
Total fuel	817,623.11/10
	81,763 L
CO_2e emitted	3.25 × 81,763
	265,729.75 t
Spraying of chitosan (distributor truck):	
Total fuel	205,207.37/7000
	30 L
CO_2e emitted	3.25 × 30
	97.50 t
Compaction of soil at the base (sheep foot roller):	
Quantity of soil at the base	1× 600 × 600
	360,000 m^3
Total fuel	360,000/12
	30,000 L
CO_2e emitted	3.25 × 30,000
	97,500.00 t
Compaction of soil at the slope (side liner) (Slope compactor roller):	

Spreading of Soil (Bulldozer)	
Quantity of soil in side slopes	$1 \times 2 \times (\sqrt{4^2 + (4 \times 1.5)^2}) \times 600$
	8653.32 m^3
Total fuel	8653.32/9
	962 L
CO_2e emitted	3.25×962
	3126.50 t
Compaction of soil at slope (cover) (slope compactor roller):	
Quantity of soil in side slopes of cover	$2 \times 0.5 \times (\sqrt{(2^2 + (3 \times 2)^2}) \times 600$
	3794.73 m^3
Total fuel	3794.73/9
	422 L
CO_2e emitted	3.25×422
	1371.5 t
Compaction of soil (final cover) (smooth wheel roller):	
Quantity of soil in final cover at the top	$0.5 \times 600 \times 600$
	180,000 m^3
Total fuel	180,000/12
	15,000 L
CO_2e emitted	$3.25 \times 15{,}000$
	48,750.00 t
Total CO_2e emitted from Phase 3	**416,575.25 t**
Total CO_2e emitted from all Phases	**740,248.98 t**

References

1. Nagaraj, T.S.; Miura, N. *Soft Clay Behaviour—Analysis and Assessment*; AA Balkema: Rotterdam, The Netherlands, 2001.
2. Suganya, K.; Sivapullaiah, P.V. Compressibility of remolded and cement-treated Kuttanad soil. *J. Soils. Found.* **2019**, *60*, 697–704. [CrossRef]
3. Sabhitha, B.S.; Evangeline, Y.S. Stabilization of Kuttanad soil using calcium and sodium lignin compounds. In *Proceedings of the Indian Geotechnical Conference*; Lecture Notes in Civil Engineering; Patel, S., Solanki, C.H., Reddy, K.R., Shukla, S.K., Eds.; Springer: Singapore, 2019; Volume 136, pp. 249–258, ISBN 978-981-33-6443-1. [CrossRef]
4. Ayyar, T.S.R. Strength Characteristics of Kuttanad Clays. Ph.D. Thesis, University of Roorkee, Roorkee, India, 1996. Available online: http://refhub.elsevier.com/S0038-0806(19)30151-9/h0020 (accessed on 30 May 2023).
5. Basma, A.A.; Tuncer, E.R. Effect of lime on volume change and compressibility of expansive clays. *Transp. Res. Rec.* **1991**, *1295*, 52–61. Available online: http://onlinepubs.trb.org/Onlinepubs/trr/1991/1295/1295-007.pdf (accessed on 30 May 2023).
6. Moghal, A.A.B.; Sivapullaiah, P.V. Characterization of lime and gypsum amended class F fly ashes as liner materials. In *Geo-Frontiers 2011: Advances in Geotechnical Engineering*; American Society of Civil Engineers: Reston, VA, USA, 2011; pp. 1162–1171. [CrossRef]
7. Moghal, A.A.B.; Moghal, A.A.B. Sustainable use of low lime fly ashes in geotechnical and geoenvironmental applications. In *Geo-Congress 2012: State of the Art and Practice in Geotechnical Engineering*; American Society of Civil Engineers: Reston, VA, USA, 2012; pp. 3681–3690. [CrossRef]
8. Mohammed, S.A.S.; Moghal, A.A.B. Efficacy of nano calcium silicate (NCS) treatment on tropical soils in encapsulating heavy metal ions: Leaching studies validation. *Innov. Infrastruct. Solut.* **2016**, *1*, 21. [CrossRef]
9. Moghal, A.A.B.; Vydehi, V.; Moghal, M.B.; Almatrudi, R.; AlMajed, A.; Al-Shamrani, M.A. Effect of calcium-based derivatives on consolidation, strength, and lime-leachability behavior of expansive soil. *J. Mater. Civ. Eng.* **2020**, *32*, 04020048. [CrossRef]
10. Meeravali, K.; Rangaswamy, K.T. Compressibility and permeability characteristics of nano chemical treated Kuttanad soft-clay. *J. Emerg. Technol. Innov. Res.* **2018**, *5*, 615–620. Available online: http://www.jetir.org/papers/JETIR1803110.pdf (accessed on 30 May 2023).
11. Ashfaq, M.; Moghal, A.A.B.; Basha, B.M. Reliability-based design optimization of chemically stabilized coal gangue. *J. Test. Eval.* **2021**, *51*, 20210176. [CrossRef]
12. Ashfaq, M.; Moghal, A.A.B.; Almajed, A. Sustainability benefits of utilizing coal gangue as fill material in earthworks. In Proceedings of the Geo-Congress 2022, Charlotte, NC, USA, 20–23 March 2022; ASCE Geotechnical Special Publication No. 335. pp. 453–462. [CrossRef]
13. Sruthi, P.L.; Reddy, P.H.P.; Moghal, A.A.B. Swelling behavior of alkali transformed kaolinitic clays treated with flyash and ground granulated blast furnace slag. *Ind. Geotech. J.* **2022**, *52*, 145–160. [CrossRef]

14. Ashfaq, M.; Moghal, A.A.B.; Basha, B.M. The sustainable utilization of coal gangue in geotechnical and geoenvironmental applications. *J. Hazard. Toxic Radioact. Waste* **2022**, *26*, 03122003. [CrossRef]
15. Moghal, A.A.B.; Sanaulla, P.F.; Mohammed, S.A.S.; Rasheed, R.M. Leaching test protocols to evaluate contaminant response of nano-calcium silicate–treated tropical soils. *J. Hazard. Toxic Radioact. Waste* **2023**, *27*, 04023002. [CrossRef]
16. Rehman, A.U.; Moghal, A.A.B. The influence & optimisation of treatment strategy in enhancing semi-arid soil geotechnical properties. *Arab. J. Sci. Eng.* **2018**, *43*, 5129–5141. [CrossRef]
17. Harsh, H.; Moghal, A.A.B.; Rasheed, R.M.; Almajed, A. State-of-the-art review on the role and applicability of select nano-compounds in geotechnical and geoenvironmental applications. *Arab. J. Sci. Eng.* **2023**, *48*, 4149–4173. [CrossRef]
18. Moghal, A.A.B.; Chittoori, B.C.S.; Basha, B.M. Effect of fiber reinforcement on CBR behavior of lime-blended expansive soils: Reliability approach. *Road Mater. Pavement Des.* **2018**, *19*, 690–709. [CrossRef]
19. Syed, M.; Moghal, A.A.B.; Chittoori, B.C.S. Reliability analysis of polyvinyl alcohol fiber-reinforced soft subgrade soil treated with lime and alkali activated stabilizer: A comparative study. In Proceedings of the Geo-Congress 2023, Los Angeles, CA, USA, 26–29 March 2023; pp. 422–432. [CrossRef]
20. Moum, J.; Rao, C.N.; Ayyar, T.S.R. A natural 17Å montmorillonite-organic complex from alleppey, Kerala State-India. *Clays Clay Miner.* **1973**, *21*, 89–95. [CrossRef]
21. Suganya, K.; Sivapullaiah, P.V. Role of composition and fabric of Kuttanad clay: A geotechnical perspective. *Bull. Eng. Geol. Environ.* **2017**, *76*, 371–381. [CrossRef]
22. Rasheed, R.M.; Moghal, A.A.B. Critical appraisal of the behavioral geo-mechanisms of peats/organic soils. *Arab. J. Geosci.* **2022**, *15*, 1123. [CrossRef]
23. Rajasekaran, G.; Essaku, S.; Mathews, P.K. Physico-chemical and mineralogical studies on Cochin marine clays. *Ocean Eng.* **1994**, *21*, 771–780. [CrossRef]
24. Lekha, K.R.; Kavitha, V. Coir geotextile reinforced clay dykes for drainage of low-lying areas. *Geotext. Geomembr.* **2006**, *24*, 38–51. [CrossRef]
25. Bindu, J.; Vinod, P. Mini-plate load test on preloaded Kuttanad clays. In Proceedings of the Indian Geotechnical Conference 2008, Bangalore, India, 1–19 December 2008.
26. Isaac, D.S.; Girish, M.S. Suitability of different materials for stone column construction. *Electron. J. Geotech. Eng.* **2009**, *14*, 2–12.
27. Shaheema, S.; Aparna, S.J. Effect of lime column on the geotechnical properties of kuttanadu soil along radial direction. *Int. J. Eng. Trends Technol.* **2016**, *39*, 260–266. [CrossRef]
28. Greeshma, P.G.; Joseph, M. Rice straw reinforcement for Improvement in Kuttanad Clay. In Proceedings of the Indian Geotechnical Conference 2011, Kochi, India, 15–17 December 2011.
29. Anupama, P.L.; Joseph, M. Improvement of Kuttanad clay using lime and fly ash—A comparative study. In Proceedings of the Indian Geotechnical Conference 2012, Delhi, India, 13–15 December 2012.
30. Moghal, A.A.B.; Vydehi, K.V. State-of-the-art review on the efficacy of xanthan gum and guar gum inclusion on the engineering behavior of soils. *Innov. Infrastruct. Solut.* **2021**, *6*, 108. [CrossRef]
31. Arab, M.G.; Rohy, H.; Zeiada, W.; Almajed, A.; Omar, M. One-phase EICP biotreatment of sand exposed to various environmental conditions. *J. Mater. Civ. Eng.* **2021**, *33*, 04020489. [CrossRef]
32. Moghal, A.A.B.; Rasheed, R.M.; Mohammed, S.A.S. Sorptive and desorptive response of divalent heavy metal ions from EICP-treated plastic fines. *Ind. Geotech. J.* **2022**, *53*, 315–333. [CrossRef]
33. Arab, M.G.; Mousa, R.A.; Gabr, A.R.; Azam, A.M.; El-Badawy, S.M.; Hassan, A.F. Resilient behavior of sodium alginate–treated cohesive soils for pavement applications. *J. Mater. Civ. Eng.* **2019**, *31*, 04018361. [CrossRef]
34. Vydehi, K.V.; Moghal, A.A.B. Effect of biopolymeric stabilization on the strength and compressibility characteristics of cohesive soil. *J. Mater. Civ. Eng.* **2022**, *34*, 04021428. [CrossRef]
35. Chang, I.; Prasidhi, A.K.; Im, J.; Cho, G.C. Soil strengthening using thermo-gelation biopolymers. *Constr. Build. Mater.* **2015**, *77*, 430–438. [CrossRef]
36. Chang, I.; Prasidhi, A.K.; Im, J.; Cho, G.C. Effects of Xanthan gum biopolymer on soil strengthening. *Constr. Build. Mater.* **2015**, *74*, 65–72. [CrossRef]
37. Smitha, S.; Sachan, A. Use of agar biopolymer to improve the shear strength behavior of sabarmati sand. *Int. J. Geotech. Eng.* **2016**, *10*, 387–400. [CrossRef]
38. Acharya, R.; Pedarla, A.; Bheemasetti, T.V.; Puppala, A.J. Assessment of guar gum biopolymer treatment toward mitigation of desiccation cracking on slopes built with expansive soils. *Transp. Res. Rec.* **2017**, *2657*, 78–88. [CrossRef]
39. Ham, S.M.; Chang, I.; Noh, D.H.; Kwon, T.H.B. Muhunthan, improvement of surface erosion resistance of sand by microbial biopolymer formation. *J. Geotech. Geoenviron. Eng.* **2018**, *144*, 06018004. [CrossRef]
40. Chang, I.; Cho, G.C. Shear strength behavior and parameters of microbial gellan gum-treated soils: From sand to clay. *Acta. Geotech.* **2019**, *14*, 361–375. [CrossRef]
41. Ghasemzadeh, H.; Modiri, F. Application of novel Persian gum hydrocolloid in soil stabilization. *Carb. Polymer.* **2020**, *246*, 116639. [CrossRef]
42. Zhao, Y.; Zhuang, J.; Wang, Y.; Jia, Y.; Niu, P.; Jia, K. Improvement of loess characteristics using sodium alginate. *Bull. Eng. Geol. Environ.* **2020**, *79*, 1879–1891. [CrossRef]

43. Soldo, A.; Miletić, M.; Auad, M.L. Biopolymers as a sustainable solution for the enhancement of soil mechanical properties. *Sci. Rep.* **2020**, *10*, 267. [CrossRef]
44. Chang, I.; Lee, M.; Tran, A.T.P.; Lee, S.; Kwon, Y.M.; Im, J.; Cho, G.C. Review on biopolymer-based soil treatment (BPST) technology in geotechnical engineering practices. *Transp. Geotech.* **2020**, *24*, 100385. [CrossRef]
45. Fatehi, H.; Ong, D.E.; Yu, J.; Chang, I. Biopolymers as green binders for soil improvement in geotechnical applications: A review. *Geoscience* **2021**, *11*, 291. [CrossRef]
46. Latifi, N.; Horpibulsuk, S.; Meehan, C.L.; Majid, M.Z.A.; Tahir, M.M.; Mohamad, E.T. Improvement of problematic soils with biopolymer—An environmentally friendly soil stabilizer. *J. Mater. Civ. Eng.* **2017**, *29*, 04016204. [CrossRef]
47. Abd, T.A.; Fattah, M.Y.; Aswad, M.F. Strengthening of soft soil using caboxymethyl cellulose biopolymer. In Proceedings of the International Conference of Al-Esraa University College for Engineering Sciences (ICAUC_ES 2021), Baghdad, Iraq, 3–4 November 2021; IOP Conference Series: Earth and Environmental; IOP Publishing: Bristol, UK, 2021; Volume 961, p. 012030. [CrossRef]
48. Tran, K.M.; Bui, H.H.; Kodikara, J.; Sánchez, M. Soil curling process and its influencing factors. *Can. Geotech. J.* **2019**, *57*, 408–422. [CrossRef]
49. Singh, S.P.; Das, R. Geoengineering properties of expansive soil treated with Xanthan gum biopolymer. *Geomech. Geoeng.* **2019**, *15*, 107–122. [CrossRef]
50. Liu, Y.; Jia, J.; Zhang, H.; Sun, S. Enhanced Cr (VI) stabilization in soil by chitosan/bentonite composites. *Ecotox. Environ. Saf.* **2022**, *238*, 113573. [CrossRef]
51. Mola, A.; Abasiyan, S.; Dashbolaghi, F.; Mahdavinia, G.R. Chitosan cross-linked with κ-carrageenan to remove cadmium from water and soil systems. *Environ. Sci. Pollut. Res.* **2019**, *26*, 26254–26264. [CrossRef]
52. Kamari, A.; Pulford, I.D.; Hargreaves, J.S.J. Chitosan as a potential amendment to remediate metal contaminated soil—A characterization study. *Colloid. Surf. B* **2011**, *82*, 71–80. [CrossRef]
53. Zinchenko, A.; Sakai, T.; Morikawa, K.; Nakano, M. Efficient stabilization of soil, sand, and clay by a polymer network of biomass-derived chitosan and carboxymethyl cellulose. *J. Environ. Chem. Eng.* **2022**, *10*, 107084. [CrossRef]
54. Shariatmadari, N.; Reza, M.; Tasuji, A.; Ghadir, P.; Javadi, A.A. Experimental study on the effect of chitosan biopolymer on sandy soil stabilization. In Proceedings of the 4th European Conference on Unsaturated Soils, Lisbon, Portugal, 24–26 June 2020; p. 195. [CrossRef]
55. Hataf, N.; Ghadir, P.; Ranjbar, N. Investigation of soil stabilization using chitosan biopolymer. *J. Clean. Product.* **2018**, *170*, 1493–1500. [CrossRef]
56. Kang, X.; Bate, B.; Chen, R.P.; Yang, W.; Wang, F. Physicochemical and mechanical properties of polymer-amended kaolinite and fly ash–kaolinite mixtures. *J. Mater. Civ. Eng.* **2019**, *31*, 04019064. [CrossRef]
57. Kannan, G.; Sujatha, E.R. Crustacean polysaccharides for the geotechnical enhancement of organic silt: A clean and green alternative. *Carb. Polym.* **2023**, *299*, 120227. [CrossRef]
58. *ASTM D854-14*; Standard Test Method for Specific Gravity of Soil Solids by Water Pycnometer. ASTM International: West Conshohocken, PA, USA, 2016. Available online: https://www.astm.org/d0854-14.html (accessed on 20 August 2022).
59. *ASTM D4318-17e1*; Standard Test Methods for Liquid Limit, Plastic Limit, and Plasticity Index of Soils. American Society for Testing and Materials: Philadelphia, PA, USA, 2018. Available online: https://www.astm.org/10.1520/D4318-17E01 (accessed on 20 August 2022).
60. *ASTM D2487*; Standard Practice for Classification of Soils for Engineering Purposes (Unified Soil Classification System). ASTM International: West Conshohocken, PA, USA, 2017. Available online: https://www.astm.org/d2487-11.html (accessed on 20 August 2022).
61. *ASTM D698-12*; Standard Test Methods for Laboratory Compaction Characteristics of Soil Using Standard Effort (12 400 ft-lbf/ft3 (600 kN-m/m^3)). American Society for Testing and Materials: Philadelphia, PA, USA, 2014. Available online: https://www.astm.org/10.1520/D0698-12R21 (accessed on 20 August 2022).
62. *AASHTO T 267*; Standard Method of Test for Determination of Organic Content in Soils by Loss on Ignition. ASTM International: West Conshohocken, PA, USA, 1986.
63. Aguilar, R.; Nakamatsu, J.; Ramírez, E.; Elgegren, M.; Ayarza, J.; Kim, S.; Pando, M.A.; Ortega-San-Martin, L. The potential use of chitosan as a biopolymer additive for enhanced mechanical properties and water resistance of earthen construction. *Construct. Build. Mater.* **2016**, *114*, 625–637. [CrossRef]
64. Adamczuk, A.; Jozefaciuk, G. Impact of chitosan on the mechanical stability of soils. *Molecules* **2022**, *27*, 2273. [CrossRef]
65. *ASTM D2435*; Standard Test Methods for One-Dimensional Consolidation Properties of Soils Using Incremental Loading. ASTM International: West Conshohocken, PA, USA, 2004. Available online: https://www.astm.org/d2435-04.html (accessed on 20 August 2022).
66. *BS 1377*; Soils for Civil Engineering Purposes—Part 1: General Requirements and Sample Preparation. British Standards Institution: London, UK, 1990.
67. Hammond, G.; Jones, C. *Inventory of Carbon & Energy: ICE*; Sustainable Energy Research Team, Department of Mechanical Engineering, University of Bath: Bath, UK, 2008; p. 5.
68. Hammond, G.; Jones, C.; Lowrie, E.F.; Tse, P. Embodied carbon. In *The Inventory of Carbon and Energy (ICE)*; Version (2.0); BSRIA: Bracknell, UK, 2011. Available online: http://www.emccement.com/pdf/Full-BSRIA-ICE-guide.pdf (accessed on 28 April 2023).

69. Moghal, A.A.B.; Obaid, A.A.K.; Al-Refeai, T.O.; Al-Shamrani, M.A. Compressibility and durability characteristics of lime treated expansive semiarid soils. *J. Test. Eval.* **2015**, *43*, 254–263. [CrossRef]
70. Moghal, A.A.B.; Obaid, A.; Al-Refeai, T. Effect of accelerated loading on the compressibility characteristics of lime treated semiarid soils. *J. Mater. Civ. Eng.* **2014**, *26*, 1009–1016. [CrossRef]
71. Rasheed, R.M.; Moghal, A.A.B.; Rambabu, S.; Almajed, A. Sustainable assessment and carbon footprint analysis of polysaccharide biopolymer-amended soft soil as an alternate material to canal lining. *Front. Environ. Sci.* **2023**, *11*, 1214988. [CrossRef]
72. Cabalar, A.F.; Awraheem, M.H.; Khalaf, M.M. Geotechnical properties of a low-plasticity clay with biopolymer. *J. Mater. Civ. Eng.* **2018**, *30*, 04018170. [CrossRef]
73. Kwon, Y.M.; Chang, I.; Cho, G.C. Consolidation and swelling behavior of kaolinite clay containing xanthan gum biopolymer. *Acta Geotech.* **2023**, *18*, 3555–3571. [CrossRef]
74. Oliveira, P.J.V.; Reis, M.J. Effect of the organic matter content on the mechanical properties of soils stabilized with Xanthan gum. *Appl. Sci.* **2023**, *13*, 4787. [CrossRef]
75. Zhang, J.; Xia, W.; Liu, P.; Cheng, Q.; Tahi, T.; Gu, W.; Li, B. Chitosan modification and pharmaceutical/biomedical applications. *Mar. Drugs* **2010**, *8*, 1962–1987. [CrossRef]
76. Kannan, G.; O'Kelly, B.C.; Sujatha, E.R. Geotechnical investigation of low-plasticity organic soil treated with nano-calcium carbonate. *J. Rock Mech. Geotech. Eng.* **2023**, *15*, 500–509. [CrossRef]
77. Vydehi, K.V.; Moghal, A.A.B.; Rasheed, R.M. Shrinkage characteristics of biopolymer treated expansive soil. In Proceedings of the Geo-Congress 2022, Charlotte, NC, USA, 20–23 March 2022; Volume 331, pp. 92–99. [CrossRef]
78. El Hadrami, A.; Adam, L.R.; El Hadrami, I.; Daayf, F. Chitosan in plant protection. *Mar. Drug.* **2010**, *8*, 968–987. [CrossRef]
79. Fernández, M.; Pagnussat, L.A.; Borrajo, M.P.; Bravo, J.J.P.; Francois, N.J.; Creus, C.M. Chitosan/starch beads as bioinoculants carrier: Long-term survival of bacteria and plant growth promotion. *Appl. Microbiol. Biotechnol.* **2022**, *106*, 7963–7972. [CrossRef]
80. Onyelowe, K.C.; Ebid, A.M.; Hanandeh, S.; Moghal, A.A.B.; Onuoha, I.C.; Obianyo, I.I.; Liberty, U.S.; Ubachukwu, O.A. The influence of fines on the hydro-mechanical behavior of sand for sustainable compacted liner and sub-base construction applications. *Asian J. Civ. Eng.* **2023**. [CrossRef]
81. Tang, C.S.; Shi, B.; Liu, C.; Suo, W.B.; Gao, L. Experimental characterization of shrinkage and desiccation cracking in the thin clay layer. *Appl. Clay. Sci.* **2011**, *52*, 69–77. [CrossRef]
82. Vydehi, K.V.; Moghal, A.A.B.; Basha, B.M. Reliability-based design optimization of biopolymer-amended soil as an alternative landfill liner material. *J. Hazard. Tox. Radioact. Waste* **2022**, *26*, 04022011. [CrossRef]
83. Ashfaq, M.; Lal, M.H.; Moghal, A.A.B.; Murthy, V.R. Carbon footprint analysis of coal gangue in geotechnical engineering applications. *Ind. Geotech. J.* **2020**, *50*, 646–654. [CrossRef]
84. Varsha, B.; Moghal, A.A.B.; Rehman, A.U.; Chittoori, B.C.S. Shear, consolidation characteristics and carbon footprint analysis of clayey soil blended with calcium lignosulphonate and granite sand for earthen dam application. *Sustainability* **2023**, *15*, 6117. [CrossRef]
85. Amulya, G.; Moghal, A.A.B.; Almajed, A. Sustainable binary blending for low-volume roads—Reliability-based design approach and carbon footprint analysis. *Materials* **2023**, *16*, 2065. [CrossRef]
86. Riofrio, A.; Alcivar, T.; Baykara, H. Environmental and economic viability of chitosan production in Guayas-Ecuador: A robust investment and life cycle analysis. *ACS Omega* **2021**, *6*, 23038–23051. [CrossRef] [PubMed]
87. Kecojevic, V.; Komljenovic, D. Impact of bulldozer's engine load factor on fuel consumption, CO_2 emission, and cost. *Am. J. Environ. Sci.* **2011**, *7*, 125–131. [CrossRef]
88. Kiliç, R.; Küçükali, O.; Ulamiş, K. Stabilization of high plasticity clay with lime and gypsum (Ankara, Turkey). *Bull. Eng. Geol. Environ.* **2016**, *75*, 735–744. [CrossRef]
89. Prusinski, J.R.; Bhattacharja, S. Effectiveness of Portland cement and lime in stabilizing clay soils. *Transp. Res. Rec.* **1999**, *1652*, 215–227. [CrossRef]
90. Sharma, H.D.; Dukes, M.; Olsen, D.M. Field measurements of dynamic moduli and poisson's ratios of refuse and underlying soils at a landfill site. *Int. J. Rock Mech. Min. Sci. Geomech. Abstr.* **2009**, *28*, 1991. [CrossRef]

Disclaimer/Publisher's Note: The statements, opinions and data contained in all publications are solely those of the individual author(s) and contributor(s) and not of MDPI and/or the editor(s). MDPI and/or the editor(s) disclaim responsibility for any injury to people or property resulting from any ideas, methods, instructions or products referred to in the content.